Uzbek Journal of Physics
DOI: https//doi.org/10.52304/.v25i2.431

Solar-pumped fiber laser without focusing and sun-tracking systems

A.G. Kakhkhorov, A.A. Sherniyozov*, Sh.D. Payziyev

Institute of Ion-plasma and laser technologies AN RUz, Durmon yuli str. 33, 100125, Tashkent, Uzbekistan

Received 14.06.2023, revised 20.06.2023

*Corresponding author: e-mail anvar.sherniyozov@gmail.com, Phone +998 977 221 904

Исследованы волоконные лазеры с солнечной накачкой без первичного концентратора. Разработана модель волоконных лазеров на кварцевом стекле, легированных ионами Nd^{3+}, с поперечной накачкой с помощью метода трассировки фотонов. На основе модели оценены распределение поглощенной мощности, возможные потери и эффективность накачки. Были проанализированы оцененные параметры и сделаны соответствующие выводы, которые позволяют сделать ряд предложений по улучшению конструкции волоконных лазеров с солнечной накачкой. Расчетная эффективность поглощения волоконного солнечного лазера без первичного концентратора или системы солнечного слежения составила 0.2% для волокна длиной 190 м. Выходная мощность волоконного лазера при этом составляет 40 мВт, а эффективность преобразования солнечного излучения в лазерное излучение равна 0.06%. Разработанная модель позволяет оценить общую эффективность, выходную мощность и распределение поглощения в волоконных Nd^{3+} лазерах без фокусирующей оптики, что дает возможность проводить различные исследовательские сравнения.

Ключевые слова: волоконный лазер с солнечной накачкой, кварцевое волокно, легирование неодимом, параболо-цилиндрический концентратор, сенсибилизатор родамин 6G.

We studied solar pumped fiber lasers without primary concentrator. A model of solar side-pumped Nd^{3+} doped silica fiber lasers was developed using photon tracing method. The absorbed power distribution, possible losses and the pumping efficiency are estimated using the model. We analyzed the estimated paramters and drawed conclutions which have many suggests for improved design of solar pumped fiber lasers. The absorption efficiency of a fiber solar laser without a primary concentrator or sun tracker was calculated to be 0.2% for a 190 m fiber. The output power of the fiber laser is 40 mW, and the conversion efficiency from sunlight to laser light is calculated to be 0.06%. The developed model allows one to estimate the overall efficiency, output power and absorption distribution of Nd^{3+} fiber lasers without focusing optics, enabling various investigative comparisons.

Keywords: Solar pumped fiber laser, Nd-doped silica fiber, parabolic-trough concentrator, Rhodamine 6G sensitizer.

I. Introduction

One way to hardness solar energy is to use solar lasers, which convert sunlight directly into laser radiation. Solar lasers have prospects of application in space laser communications, processing of magnesium resources, etc. [1-3]. The major obstacle to the practicality of solar lasers is the relatively low power-to-power conversion efficiency, which is observed to be around 5%. The overall efficiency of solar lasers mainly depends on the active laser medium's optical properties [4-5], the primary concentrator [6] and the secondary concentrators. In addition, the efficiency and stability of solar lasers are negatively impacted by the primary concentrator type and the solar tracking system. To overcome technical issues associated

with the primary concentrator, a solar-pumped fiber laser is proposed [7]. In 2017, a solar fiber laser immersed in a sensitizer solution was demonstrated to increase absorption efficiency and reduce the threshold pump power [8]. A 40 m long Nd^{3+} doped silica fiber was immersed in a solution of rhodamine 6G (R6G) in methanol because R6G has a high fluorescence efficiency and its fluorescence absorption spectrum coincides with the absorbtion spectrum of Nd^{3+} doped silica fiber. The limit of laser generation up to 1.5 W/cm^2 has been reached. In 2019, Endo et al. performed Monte Carlo ray tracing simulations on a fiber laser with transverse solar pumping and proved that a laser power of 1 mW can be obtained without a primary concentrator [9]. In 2020, Masuda et al. reported a transversely solar-pumped Nd^{3+} fiber laser placed in a dye-filled chamber [7]. Although the maximum output power was only 1.3 mW, according to their calculations, the efficiency of converting solar energy into laser energy can be as high as 8%.

Furthermore, solar fiber lasers are studied with primary concentrators. In 2021, Pan Guo [10] et al. chose a primary concentrator radius of 600 mm and concentrated 217.7 W of solar power in an annular chamber, which allowed 73.5 W of solar power to be absorbed by the neodymium fiber core and 21.4% overall increase in efficiency. The output power of the laser was 2.6 W, the slope efficiency was 3.7%. In 2022, Pengfei Xiang [11] et al. reported that with an input solar power of 1307.4 W, the maximum output power is showen to be 60.62 W using TracePro software for Nd:YAG crystalline fiber with a core diameter of 1mm and a length of 150 mm. The laser conversion efficiency of 4.64% is demonstrated.

Jianlei Wang [12] et al. numerically studied solar fiber lasers. They showed that maximum output power of 63.3 W and a slope efficiency of 34.2% can be achieved using a 791 nm laser diode for pumping of Tm:YAG crystal fiber. A key point from this short review is that the overall efficiency of solar-powered fiber lasers without a primary concentrator is discouragingly low. However, the reasons or mechanisms for the very low efficiency have not been sufficiently studied. More importantly, possible mechanisms, concepts and schemes for the improvement of solar-fiber lasers are not being discussed. The lack of sufficient theoretical analysis is understandable due to the complex nature of solar fiber lasers.

Therefore, we believe more theoretical and experimental research into solar fiber lasers without primary concentrators is necessary. In this regard, creating a fully functional and detailed model that accounts for significant factors is essential. Therefore, in this work, our purpose is to develop a model for Nd^{3+} doped solar fiber lasers without any primary concentrator.

II. Simulation technique

Due to the physical complexity of solar-fiber lasers and inherent randomness in solar radiation, analytical and/or numerical methods are practically unsuitable for model development. Another suitable tool is a simulation based on the ray/photon tracing concept. In general, the model can be developed by many ready-to-use ('black box') software like Zemax and TracePro, two of the most popular packages in physical optics. However, we here intend to use the so-called *photon* tracing method. The *photon* tracing can be considered a modified ray tracing method with Monte Carlo to control random processes. The versatility of *photon* tracing for modeling solar lasers is demonstrated in our previous studies [13-16].

III. Description of the hardware parts in the model

We adopted the following model specifications and parameters to develop the model. A schematic construction of the solar fiber laser is shown in Figure 1, where size rations are altered for better representation.

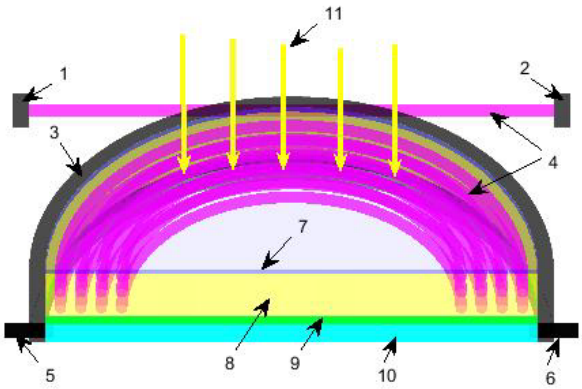


Figure 1. A typical example of a solar fiber laser. 1, 2 – resonator mirrors, 3 – outer cover, 4 – fibers as the active medium, 5, 6 – ins and outs for water, 7 – dichroic mirror, 8 – luminescent collector (rhodamine 6G), 9 – highly reflective mirror, 10 – cooling liquid, 11 – sun rays.

III.1. Cylindric cavity

A cylindric cavity with a radius of 15 cm and a height of 1.5 mm is chosen to contain all other parts

©Academy of Sciences of Republic of Uzbekistan, 2023

of the solar laser. Walls of the cavity, such as bases and inner sides, are processed with coating technology (broadband HR mirror), which is made of multiple dielectric layers. As a result, its reflectivity is equal to 96% (Figure 2). The working surface area of the base is 707 cm^2, from which solar radiation is allowed into the system. The top of the cylinder is made from a dichroic mirror (more detailed information is provided further in the text).

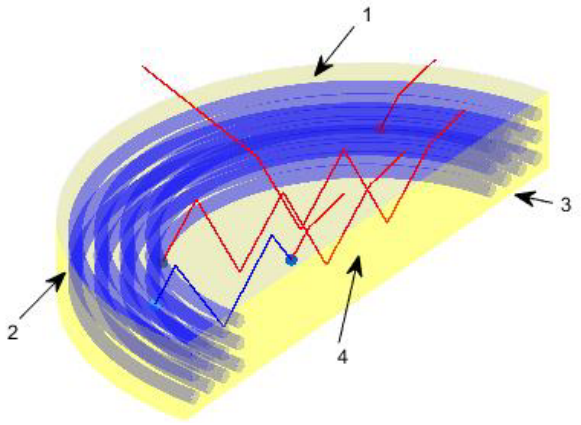


Figure 2. Schematic diagram of the path of the photon and its absorption in the fiber. 1 – dichroic mirror, 2 – side wall, 3 – bottom wall, 4 – R6G solution.

III.2. Nd^{3+} doped silica fiber

Long thin fiber with length of 190 m is coiled (lay down) inside cylindric cavity. The cross-section of the fiber consists of two parts: outer part (cladding) and inner (core) part. The core made of Nd^{3+} ions inserted silica. The diameters of the cladding and core are 125 mkm and 16 mkm, respectively. In the design of fiber coils, the minimum bend radius is taken into consideration.

III.3. R6G sensitizer

The overlap between silica fiber absorption spectrum and solar spectrum is very narrow negatively impacting the pumping efficiency. To improve this poor overlap, the cavity is filled with R6G (Rhodamine 6G, 0.3 mmol×L^{-1} solution (Sigma Aldrich). The R6G plays the role of sensitizer for Nd ions as can be seen from spectral plots in Fig. 3. The R6G can absorb the wider spectrum from 400 nm up to 587 nm peaking around 527 nm, which corresponds to 3.49 cm^{-1} or 1516 dB/m [6]. The emission spectrum of R6G is located between 501 and 796 nm, which is perfect overlaps with the highest absorption band of Nd ions in the core.

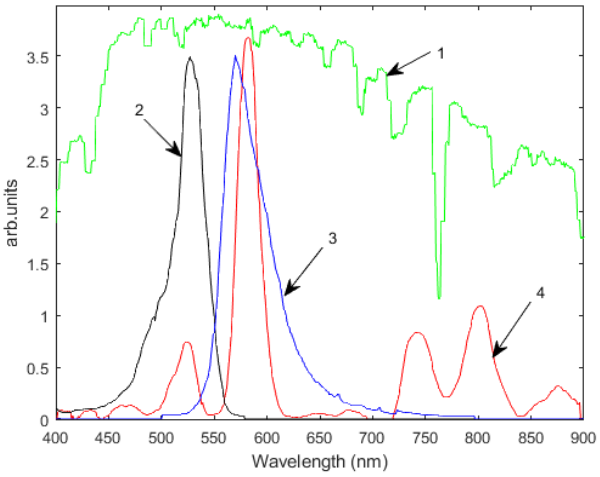


Figure 3. Standard solar spectrum (1), R6G absorption spectrum (2), R6G emission spectrum (3), fiber absorption spectrum (4).

III.4. Dichroic mirror

The cylindric cavity shown in Fig. 1 is enclosed with a dichroic mirror in the top. The purpose of the dichroic mirror is to prevent the escape of potentially absorbable photons. The mirror has near 100% reflectivity for wavelengths between 550 nm and 725 nm. This range perfectly overlaps the absorption band of Nd ions and also the emission spectrum of the sensitizer R6G (Fig. 4). Beyond the range from 550 nm and 725 nm, the mirror is almost transparent, allowing the escape of unabsorbable photons. This can help to avoid overheating of the system.

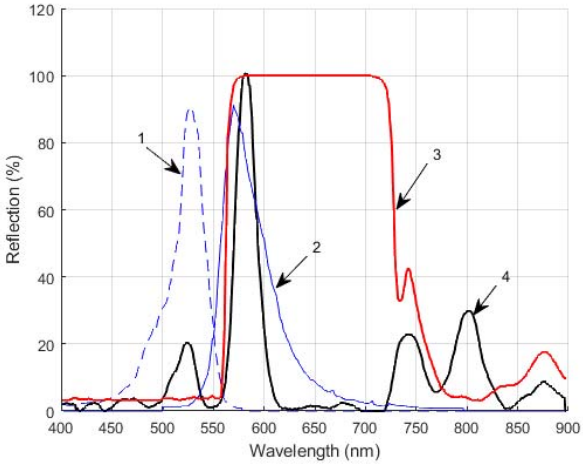


Figure 4. R6G absorption spectrum (1), R6G emission spectrum (2), dichroic mirror reflection (3), fiber absorption spectrum (4).

©Academy of Sciences of Republic of Uzbekistan, 2023

IV. The developed model

As described, 190 m long optical fiber wrapped around the axis of the cavity on a ring with a radius of 15 cm and a thickness of 1.5 mm. In the model, each fiber coil is considered as a separate ring, that is, the shape of the fiber is approximated by tori. The total length of the fiber was obtained as the sum of the lengths of the annular loops in the row and column. It consisted of 8 rows and 25 columns and 200 loops. The gap (distance) between fibers in a column and a row is assumed to be 50 μm. The gaps are filled with sensitizer since the chamber was filled with an R6G solution in methanol, which acts as a luminescent solar concentrator to shift the solar spectrum and provide better overlap with the absorption spectrum of the Nd^{3+} doped silica fiber active medium. The surface of the cavity is 707 cm^2. If the solar radiation is assumed to be 1000 W/m^2, the around 70 W solar energy enters into the cavity.

In the model, sampled solar photons enter into system. They can interact with several geometric objects: dichroic mirror (plane), fibers (torus), walls of cylinder, R6G medium. Possible trajectories and behaviors of photons in each of these system elements are followings. The dichroic mirror selectively reflects photons calculating reflection probability in terms of reflection spectrum. Fibers can reflect photons or allow them to be refracted inwards. Photons that entered onto fiber can propagate inside and hence get absorbed resulting in pumped photon.

Absorption probability of photons is calculated in terms of Nd^{3+} silica absorption spectrum. The escape of photons from fiber is also possible. The propagation of photons in R6G can result in absorption and give rise to a new photon with a new wavelength which sampled from the emission spectrum of the R6G. Coated cylinder wall has 0.96 reflectivity which is approximated value for all wavelengths. All these trajectories and behaviors are modeled and monitored to estimate the performance of the system.

V. Results and discussions

One advantage of this developed model as opposed to “black box” type modelling is that it allows us to estimate the performance of each element in the system. Taking this advantage, we calculated the power distribution of the entered solar energy among elements in the system. The results are presented in Table 1.

Table 1. Power distribution

Processes	Power (W)	Relative power (%)
Total incident photons	70.7	100
Refracted through a dichroic mirror	66.86	94.57
Those who left the dichroic mirror	26.81	37.92
Those reflected from the dichroic mirror surface	3.81	5.39
Photons that are not absorbed	30.24	42.77
Absorbed in R6G solution	7.25	10.26
Losses on a lower basis	8.74	12.37
Side wall losses	0.89	1.26
Absorbed in the fiber core	0.144	0.2
Output power	$40*10^{-3}$	0.06

Data in Table 1 shows losses at each element and at a process in the system.

The dichroic mirror. As stated above, 70.7 W solar power is incident on the system. First step in the process is the passage of photons through the dichroic mirror. It is estimated by the model that the mirror causes 5.43% loss from total power. The second loss at the mirror is 37.92 %, so in total the loss at the mirror adds up to 43.35%. At first consideration, this seems to be very significant. However, it should be noted that the mirror discharges photons which are hard to get absorbed by either Nd^{3+} silica or R6G.

R6G solution. The R6G medium can absorb 10.26% from total power. So, the “sensitizer-ness” of the medium helps to frequency-shift 7.25 W solar photons. If we consider the quantum yield of the medium, this 7.25 W value further decreases resulting in a very low “sensitizer-ness”.

Nd^{3+} silica. 0.2 % from total power is absorbed in the fiber core as a usefully pumped photons, eventually giving rise to the laser output. Here, it should be noted that 0.144 W (0.2%) is contributed by both direct solar photons and frequency-shifted photons in R6G.

Cylinder walls. Due to imperfect reflectivity (0.96) of the cavity walls, the loss at the wall is 1.26%, relatively smaller and this factor can be further mitigated by the increa-sed reflectivity.

Cylinder base. (Only lower end, upper end is not included). Even though the reflectivity is the same as the wall, the loss at the base is much higher at level of 12.37%.

©Academy of Sciences of Republic of Uzbekistan, 2023

Table 2. Power distribution.

Processes	Power (W)	Relative power (%)
Total incident photons	70.7	100
Unabsorbable Photons by both Nd^{3+} and R6G	30.23	42.77
Potentially useful/absorbable photons	40.47	57.23
Loss at the dichroic mirror	30.64	43.35
Loss at the cylinder base	8.74	12.37
Loss at the wall	0.89	1.26
Absorbed in the fiber core	0.144	0.2

Table 2 shows the total loss data for each element. Data in Tables 1 and 2, which are estimated within the developed model can yield very useful insights into the modeled system. The data clearly suggest which parts of the system design should be significantly improved. One of main findings is that the dichroic mirror needs to be improved due to significant loss at the mirror Second takeaway is the very low sensitizing ability of R6G, which indicates the need to consider other materials. Third takeaway is that loss at the base is considerable and different pumping configurations can be experimented to further decrease this loss.

Laser Output. Analyzing power distribution, losses and pumping to the core leads us to the calculation of the laser output, the ultimate performance criteria of solar pumped fiber lasers. Since active medium Nd^{3+} silica is being modelled, four energy level schemes will be used to calculate. Necessary parameters for the laser output are the saturation intensity, fiber core volume, radius of fiber core, small signal gain coefficient, pumped power in the fiber core, the reflection loss at the resonator mirrors, intrinsic loss coefficient of the active medium and the physical properties of fiber. The derivation of the working equation is not included. However, it is worth mentioning that it uses the rate equation, Boltzmann distribution, and Beer-Lambert laws [17]. So, the fiber laser output power is found using the following formula [14]: medium,

$$P_{out} = I_s V g_0 \left(1 - \sqrt{(\alpha_0 + A/L)/g_0}\right)^2,$$

where I_s is the saturation intensity, $V = \pi r^2 L = 2.01\times10^{-10} L$ – fiber core volume, r – radius of fiber core, $g_0 = (12\text{W}^{-1})\times P_{abs}(L)/L$ – small signal gain coefficient, P_{abs} – power of photons absorbed in the fiber core, A = 1.5% is the reflection loss at the resonator mirror [15], $\alpha_0 = 6.91\times10^{-4}$ m^{-1} (3 dB km^{-1}) is the intrinsic loss coefficient [4], L – length of fiber. So, we calculated that the output power for a fiber with a radius of 8 μm and a length of 190 m is equal to 40 mW. This corresponds to the efficiency of converting sunlight into laser light 0.06%. The results derived from the model and calculation method developed in this study align with the findings of another study [14], which calculated an output power of 39 mW using ray tracing modeling.

VI. Conclusion

A model of solar side-pumped Nd^{3+} doped silica fiber lasers was developed based on the Monte Carlo photon tracing method. The absorbed power distribution, possible losses and the pumping efficiency are estimated using the model. We analyzed the estimated paramters and drawed conclusions which have many suggests for improved design of solar pumped fiber lasers. The absorption efficiency of a fiber solar laser without a primary concentrator or sun tracker was calculated to be 0.2% for a 190 m fiber. The output power of the fiber laser is 40 mW, and the conversion efficiency from sunlight to laser light is calculated to be 0.06%. The developed model can be used to theoretically analyze and optimize the solar pumped fiber lasers.

Acknowledgement. We would like to express our sincere gratitude to prof. Masamori Endo for his support in the initiation of the current study.

References

[1] G. Duncan. Nat. Photonics **4**, 64–65 (2010), https://doi.org/10.1038/nphoton.2009.272

[2] T. Saiki, S. Taniguchi, K. Nakamura, and Y. Iida. Electr. Eng. Jpn. **199**, 3-9 (2017). https://doi.org/10.1002/eej.22961

[3] M. Vasile and C.A. Maddock. Adv. Space Res. **50**, 891-900 (2012), https://doi.org/10.1016/j.asr.2012.06.001.

[4] C.R. Vistas, D. Liang, J. Almeida, B.D. Tibúrcio, D. Garcia, M. Catela, H. Costa, E. Guillot. J. Photonics Energy **11**, No.1, 018001 (2021). https://doi.org/10.1117/1.JPE.11.018001.

[5] D. Liang, J. Almeida, D. Garcia, B.D. Tibúcio, E. Guillot, C.R. Vistas. Sol. Energy **199**, 192-197 (2020). https://doi.org/10.1016/j.solener.2020.02.027.

[6] A. Sherniyozov, S. Payziyev. Uzbek Journal of Physics **21**, (4), 245-249 (2019). Retrieved from http://ufj.uz/index.php/ufj/article/view/113.

[7] T. Masuda, M. Iyoda, Y. Yasumatsu, S. Dottermusch, I.A. Howard, B.S. Richards, J.F. Bisson, M. Endo. Commun. Phys. **3**, No.1, 60 (2020). https://doi.org/10.1038/s42005-020-0326-2

©Academy of Sciences of Republic of Uzbekistan, 2023

[8] T. Masuda, M. Iyoda, Y. Yasumatsu, M. Endo. Opt. Lett. **42**, No. 17, 3427–3430 (2017). https://doi.org/10.1364/OL.42.003427
[9] M. Endo, J.F. Bisson, T. Masuda. Jpn. J. Appl. Phys. **58**, 112006 (2019). DOI 10.7567/1347-4065/ab4a93
[10] Pan Guo, Mingyu Ou, Yan Liu, Yulong Tang, Jun Zhou, LanLing Lan. International Journal for Light and Electron Optics **247**, 167933 (2021). https://doi.org/10.1016/j.ijleo.2021.167933
[11] Pengfei Xiang, Lanling Lan, Yan Liu, Hongfei Qi, Yulong Tang, Xiuhua Ma. Applied Optics **61**, No.30 (2022). https://doi.org/10.1364/AO.471537
[12] J. Wang, J. Dong, J. Liu, Z. Wang, X. Xu, Y. Xue, J. Xu, C. Wang, and Y. Zhao. Opt Express **30**, 29015-29021 (2022). https://doi.org/10.1364/OE.465790
[13] A. Sherniyozov, M. Ismailov, G. Khalikov, S. Payziyev. Uzbek Journal of Physics **21**, No.6, 370-374 (2019). https://doi.org/10.52304/.v21i6.144
[14] A.A. Sherniyozov, S.D. Payziyev. Appl. Sol. Energy **56**, 458-465 (2020). doi.org/10.3103/S0003701X20060092
[15] A.A. Sherniyozov, S.D. Payziyev. Uzbek Journal of Physics **24**, No.3, 157-162 (2022). https://doi.org/10.52304/.v24i3.357
[16] S. Payziyev, Kh. Makhmudov, and Yasser A. Abdel-Hadi. Optik **156**, 891 (2018). https://doi.org/10.1016/j.ijleo.2017.12.071
[17] W. Koechner. Solid-State Laser Engineering (Springer, Heidelberg, Germany, 1999).

Фокуслаш ва қуёшни кузатиш тизимларсиз қуёш нурлари билан дамланадиган оптик толали лазер

A.G. Kakhkhorov, A.A. Sherniyozov, Sh.D. Payziyev

Ион-плазма ва лазер технологиялари институти, Дўрмон йўли кўчаси 33, 100125, Тошкент, Ўзбекистон

Бирламчи концентраторсиз қуёш билан дамланадиган толали лазерлар ўрганилди. Фотонларни кузатиш методидан фойдаланиб, қуёш билан кўндаланг дамлаш орқали Nd^{3+} қўшилган кварц толали лазерларининг модели ишлаб чиқилди. Модел ёрдамида ютилган қувват тақсимоти, мумкин бўлган йўқотишлар ва дамлаш самарадорлиги баҳоланди. Биз аниқланган параметрларни таҳлил қилдик ва қуёш нури билан ишлайдиган толали лазерларнинг дизайнини такомиллаштириш бўйича кўплаб таклифларга эга бўлган хулосалар чиқардик. Бирламчи концентратор ёки қуёш кузатувисиз толали қуёш лазерининг умумий самарадорлиги 190 м тола учун 0.2% эканлиги топилди. Толали лазернинг чиқиш қуввати 40 мВт, қуёш нурини лазер нурига айлантириш самарадорлиги эса 0.06% ни ташкил қилади. Ишлаб чиқилган модел Nd^{3+} толали лазерларнинг умумий самарадорлигини, чиқиш қувватини ва ютилиш тақсимотини баҳолаш имконини беради, бу эса турли тадқиқот таққослашларини амалга ошириш имконини беради.

Калит сўзлар: қуёш билан оптик дамланадиган толали лазер, неодим қўшилган кварц тола, параболо-цилиндрик концентратор, родамин 6G сенсибилизатори.

©Academy of Sciences of Republic of Uzbekistan, 2023